Synopsis of Thesis research work

(within 5000 words)

Title: Study of Electronic Structure, Optical and Magnetic Response of the Disordered Solids

Submitted by: Banasree Sadhukhan

Supervisor: Prof. Arabinda Nayak

Institution: Presidency University
Department of Physics, 86/1 College Street,
Kolkata-700073, India

Reg. No : R-14RS09240062
Email : banasree.rs@presiuniv.ac.in / banasree.sadhukhan@gmail.com
Degree for which submitted: Doctor of Philosophy
Date of Registration : 12/08/2016

Prof. Arabinda Nayak
(Signature of Supervisor)

Banasree Sadhukhan
(Signature of Candidate)

1 Introduction

Prior to the rapid expansion of research in the sixties of the last century, a large majority of the theoretical studies of solids dealt with solids with constituent atoms sitting on perfect lattices. Their success was based on the theorem of Bloch, which extracted from the lattice translation symmetry of the underlying Hamiltonian. There are some systems where potential periodicity breaks down in particular directions, e.g. at surfaces and interfaces. Or periodicity may be broken in the bulk, as in amorphous materials, glasses, defects, spin glasses, molecular clusters, micro-crystallites, etc. There are some other systems where crystals having a perfect lattice structure, the lattice positions were randomly occupied by constituent atoms. Examples are solids with chemical impurities, voids and such extraneous implants. Random alloys also belong to this category. Disorder in solids can be structural or substitutional. Although both types of disorder are often relevant, we have focussed on disordered, binary substitutional alloys : A_xB_{1-x}, where A and B are the constituent atoms and x is the atomic percentage of A. Chemical disorder may involve substitutional alloys where constituent atoms B randomly replaces A atoms on an undistorted lattice. It may also involve interstitial alloys, where constituent atoms B randomly occupy previously empty interstitial sites. The thrust of the thesis is on the study of electronic structure, optical and magnetic response of such disordered systems.

The study of response function of an alloy system to external disturbances provides us many useful information about its microscopic structure. In particular, the study of optical response of a solid is one of the most powerful tools to analyze the system. It provides much useful information about the electronic energy structure through the response of the mobile electrons to an external oscillating electronic field. The optical response of the solid material is characterized by the complex refractive index, which can be expressed in terms of two optical functions, namely, the complex dielectric function and the optical absorption coefficient (or the optical conductivity). These quantities are frequency-dependent functions and are directly related to the energy band structure of solids. There have been a number of works done on light-solid state interactions. But most of the work is on a certain type of materials (like metals, semiconductors, ordered alloys) having the translation symmetry. The calculation of the properties in disorder systems is a challenging problem. Our object is to develop a formulation to study the configuration averaged optical response in binary disordered alloys.

Elementary spin excitations (magnons) play a fundamental role in modern spintronics. The challenge of spintronics research is to explore the nature of the magnon dispersion spectrum and spin transport in pristine metals, semiconductors and their alloys. Simultaneously, the synthesis of magnons in complex, low-dimensional ferromagnetic oxide and nanostructures has become a reality. Magnons also play a fundamental role in many physical phenomena such as fast magnetization reversal, magnetic ordering, spin dynamics and current induced magnetic switching. First principles study of spin correlation functions and magnon lifetimes of disordered magnetic systems have become important because of both fundamental and technological interest. Our aim to study magnetization dynamics in disordered alloys.

2 Methodology and computational details

To deal such kinds of disorder, configuration averaging of physical quantities is most important and difficult to calculate. The Coherent Potential Approximation (CPA) has been one of the most successful techniques in evaluating configuration averaging. However it is single-site mean field approximation. It cannot accurately take into account the local correlations leading to clustering or short-ranged ordering. With the realization of the need to go beyond the CPA, several attempts have been reported. These include the nonlocal CPA (NL-CPA) [1], the special quasirandom structures (SQS) [2], the locally self-consistent multiple scattering approach (LSMS) [3], traveling cluster approximation (TCA) [4], the itinerant coherent potential approximation (ICPA) [5] and Augmented Space Recursion (ASR) [6] - [11]. The ASF has proved to be one of the most powerful techniques, which can accurately take into account the effects of correlated fluctuations arising out of the disorder in the local environment. In fact, the Augmented Space Formalism (ASF) is the basis upon which the NL-CPA, the TCA, the LSMS, the ICPA and the ASR were originally developed. It includes the effects of local lattice distortion, short-range ordering due to local chemistry, the phonon problem with essential off-diagonal disorder in the dynamical matrices, and electrical and thermal transport properties in disordered alloys.

We have presented a real-space formulation for calculating the electronic structure and response functions of such random alloys based on the Kubo linear response theory interfaced with the augmented space recursion (ASR) formulated with the Tight-binding Linear Muffin-tin Orbitals (TB-LMTO) basis. The computationally feasible technique seamlessly combines three approaches : the density functional based linear muffin-tin orbitals (LMTO) for self-consistently obtaining a sparse Hamiltonian; the generalized recursion method to obtain the one and two-particle Green functions and augmented space approach to deal with disorder averaging. We have used LDA correlation energy parameterized by van Barth and Hedin [12]. To address the band gap problem for, we have used local-density approximation (LDA) modified with van Leeuwen-Baerends (vLB) correction [13] to exchange part. The correction give a substantial improvement in the band gaps over the LDA. To assess the optical conductivity of disorder system, we use Kubo-Greenwood approach (KGA) [14], [15] with ASR technique. The KGA-ASR technique is used for systematic study of band gap tuning and configuration averaged optical responses in random alloys, which can be a unique formalism for calculating optical response of semiconducting alloys, both bulk and finite size. The detail numerical derivation is presented in Appendix.

The ASR method is a real-space technique for treating random disorder of alloys. Recursion needs a countable basis $\{|n>\} \in Z^d$, which is provided by the TB-LMTO basis with n labelling the atomic positions $\vec{R}_n$. Since the ASR deals with the space of configuration fluctuations, e.g. for binary randomness $\Pi^{\otimes}\ Z_n^2$, thus Bloch's theorem plays no role. The ASR (TB-LMTO) calculations were done self-consistently and non-relativistically for given experimental geometry till the "averaged relative error" between the converged final and the previous iteration charge density and energy is reached, i.e. 10^{-5} and 10^{-4} Ryd/atom respectively. We use the tetrahedron method for k-space integration, and Anderson mixing to facilitate convergence. In TB-LMTO-vLB core states are treated as atomic-like in a frozen-core approximation and energetically higher-lying valence states are addressed in the self-consistent calculations of the effective crystal potential, which is

constructed by overlapping Wigner-Seitz spheres for each atom in the unit cell.

3 The aim of the thesis and its achievements in that perspective

3.1 Effect of random vacancies on the electronic properties of graphene and T graphene

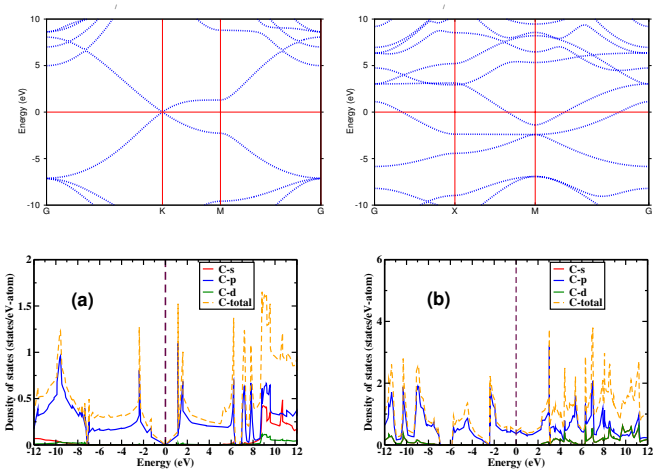

Figure 1: (Color Online) The band structure (BS) and density of states (DOS) of (left panel) graphene and (right panel) planar T graphene. The Fermi level is set to 0 eV. The linear dispersion appears due to the crossing of two opposite cones at K point in the band structure (BS) in graphene whereas planar T graphene is metallic.

We have studied the effect of random vacancies on pristine graphene and planar T graphene from both real and reciprocal space approaches. Graphenes are allotropes of carbon in which the carbon atoms are arranged in a two-dimensional (2D) honeycomb lattice, and are the building blocks of many multi-functional nano-materials. Ever since its discovery there has been keen interest in graphene because of its unconventional low-energy behavior : half-integer Hall effect, ultra-high electron mobility, low resistivity, ballistic electronic conductivity and massless carriers. The unique properties of graphene arise from its linear dispersion around the Dirac point. This is attributed to the crossing of π and π^* bands at the K and K' points of the Fermi energy level in the reciprocal space. As a result, graphene is a zero-gap semiconductor. In Dirac points the effective mass is equal to zero. T graphene is an another allotrope of carbon atoms which is composed of a periodic array of tetragonal and octagonal (4,8) carbon rings [16]. It can be produced by cleaving two adjacent atomic layers in a body-centred cubic C_8 or trigonal C_4 along the (001) direction. The linear dispersion appears at Dirac point for graphene. Whereas for planar T graphene, the π and π^* does not induce linear dispersion at Fermi level and hence, the band structure becomes metal-like as shown in Fig.1. We have inserted random vacancies at different concentrations, to simulate disorder in pristine graphene and planar T graphene sheets. The resulting disorder, both on-site (diagonal disorder) as well as in the hopping integrals (off-diagonal disorder), introduces sharp peaks in the vicinity

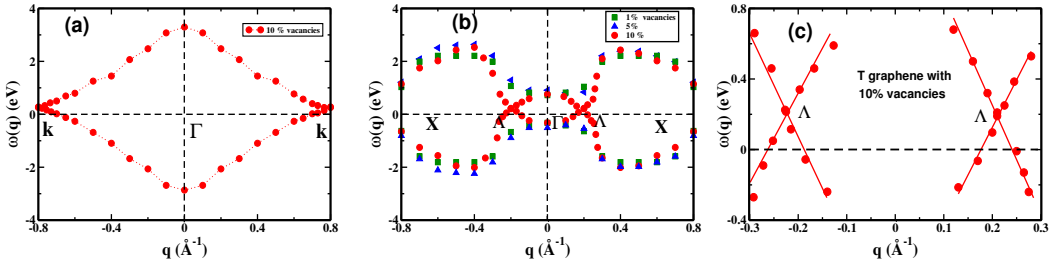

Figure 2: (Color Online) π - $\pi*$ band structure (BS) near the Fermi level in the first brillouin zone for both (a) graphene and (b) and (c) planar T graphene with 10% vacancy. With 10% vacancy concentration, T graphene induces dirac dispersion like graphene. The Fermi energy $\mathbf{E_F}$ is at 0 eV.

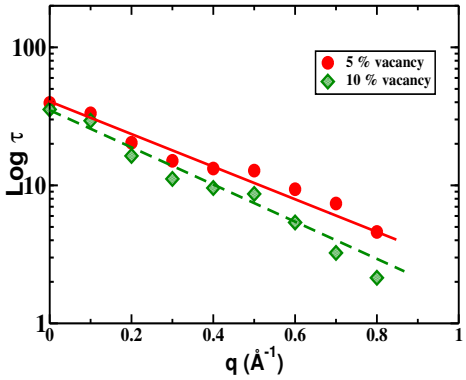

Figure 3: (Colour online) Relaxation time of graphene between the Γ and k points with random vacancies from disordered induced self energy Σ_{e-e}.

of the Dirac point built up from localized states for both hexagonal and non-hexagonal structures. These peaks become resonances with increasing vacancy concentration. We find that in presence of vacancies, graphene-like linear dispersion appears in planar T graphene and the cross points form a loop in the first Brillouin zone similar to buckled T graphene that originates from π and π^* bands without regular hexagonal symmetry (see Fig.2). We also calculate the single-particle relaxation time, $\tau(\vec{q})$ of $\vec{q}$ labeled quantum electronic states which originates from scattering due to presence of vacancies, causing quantum level broadening.

From a many-body-theory viewpoint the single particle relaxation time $\tau(\vec{q})$ is calculated from the electron self energy of the coupled electron-impurity system. The configuration averaged Green function is

$$\ll G(\vec{q},z) \gg = g(\vec{q},z) + g(\vec{q},z)\Sigma(\vec{q},z)G(\vec{q},z)$$

The averaged spectral function is

$$\begin{aligned} A(\vec{q},z) &= -\frac{1}{\pi}\,\Im m \ll G(\vec{q},z) \gg \\ &= \frac{\Sigma_{im}(\vec{q},z)/\pi}{(g^{-1}(\vec{q},z)-\Sigma_{real}(\vec{q},z))^2+(\Sigma_{im}(\vec{q},z))^2} \end{aligned} \tag{1}$$

This $\Sigma_{im}(\vec{q},z)) = 1/\tau$ is the disorder induced lifetime of a $\vec{q}$ labeled quantum state. We obtain disorder induced lifetime τ of a $\vec{q}$ labeled quantum state from the Fourier transform of the configuration averaged self energy function. Fig.3 shows the calculated single particle relaxation time $\tau(\vec{q})$ as a function of $\vec{q}$ $(\mathring{A}^{-1})$ in first Brillouin Zone for graphene. The relaxing modes or patterns are labeled by $\vec{q}$, such that the average 'size' of the mode is $O(q^{-1})$. We define the lifetime $\tau(\vec{q})$ as the time in which the disordered induced self energy amplitude drops to its $1/e$ value. The central impurity peak is increasing with increasing vacancies (disorder). Log $\tau(\vec{q})$ decreases almost linearly with increasing wave vector $\vec{q}$. Relaxation time $(\tau(\vec{q}))$ decreases with increasing disorder strength. Disorder-induced broadening is related to the scattering length (or life-time) of Bloch electrons. We believe that such a study may provide a useful insight into the scattering mechanism of disordered graphene.

Finally, we believe that our framework is suitable for the study of the effects of disorder in other 2D materials such Silicene, boron nitride mono layer.

3.2 Effect of disorder on the optical response of NiPt and Ni_3Pt alloys

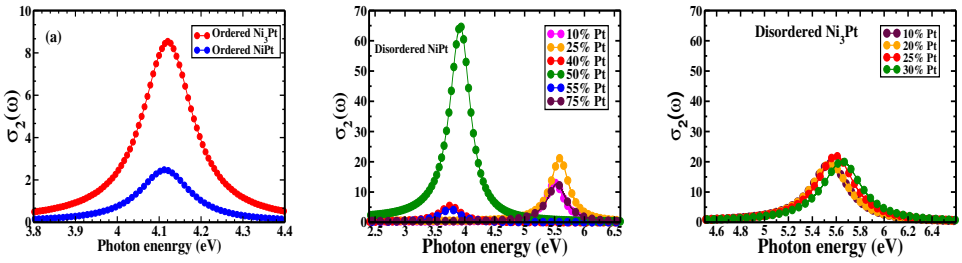

Figure 4: (Color Online) The imaginary part $\sigma_2(\omega)$ of optical conductivity $\sigma(\omega)$ for (left) ordered NiPt and Ni_3Pt, (middle) Ni_xPt_{1-x} and (right) disordered $Ni_{3(1-x)/3}Pt_x$. For disordered NiPt we have used x=0.1, 0.25, 0.4, 0.5 0.55, 0.75 ie 10%, 25%, 40%, 50%, 55%, 75% and that for disordered Ni_3Pt we have used 10%, 20%, 25%, 30% Pt concentration respectively.

Transparent conductive electrodes (TCO) are indispensable components of many opto-electronic devices including solar cells, organic light emitting diodes, photodetectors, touchscreens, integrated modulators, liquid-crystal displays, electrochromic devices and photocathodes of dye synthesized solar cells. Pd (4d) and Pt (5d) rich alloy of 3d transition metals shows interesting optical and magnetic properties which open up a variety of applications. The wide optical transparency and excellent electrical properties, combined

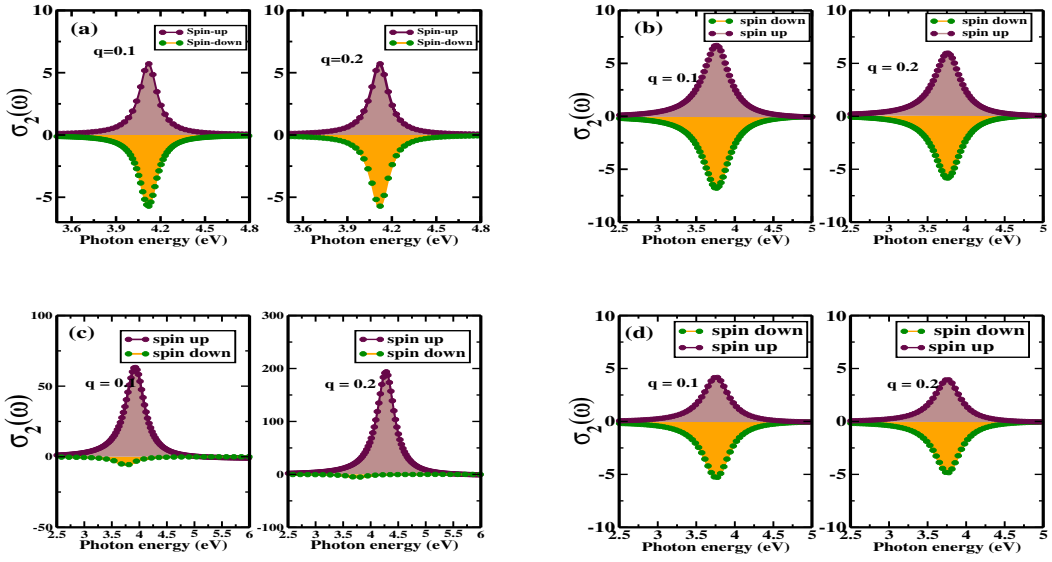

Figure 5: (Color Online) Spin resolved optical response of (a) ordered NiPt and disordered $Ni_{1-x}Pt_x$ (0.4< x <0.6) ie (b) 40%, (c) 50% and (d) 55% Pt content in disordered binary alloys. Here $\vec{q}$ is the reciprocal lattice vector defined as $\mathring{A}^{-1}$.

with the proven stability after an ad hoc passivation treatment, make Ni based ultra thin metallic films (UTMF) serious competitors to TCOs, in particular in the UV and IR spectral regions. Ni based thin alloy-films are far better than single component Ni based UTMF. The optical as well as magnetic properties of alloy films can be tailored according to requirements. We present a detailed study of the effect of chemical disorder on the optical response of $Ni_{1-x}Pt_x$ ($0.1\leq$ x ≤ 0.75) and $Ni_{3(1-x)/3}Pt_x$ ($0.1\leq$ x ≤ 0.3). We show that chemical disorder has a large impact on optical response of Ni-Pt systems. In ordered Ni-Pt alloys, the optical conductivity peaks are sharp. But as we switch on chemical disorder, the UV peak becomes broadened and its position as a function of composition and disorder carries the signature of a phase transition from NiPt to Ni_3Pt with decreasing Pt concentration. Quantitatively this agrees well with Massalski's Ni-Pt phase diagram [17]. Both ordered NiPt and Ni_3Pt have an optical conductivity transition at 4.12 eV. But disordered NiPt has an optical conductivity transition at 3.93 eV. If we decrease the Pt content, it results a chemical phase transition from NiPt to Ni_3Pt and shifts the peak position by 1.67 eV to the ultraviolet range at 5.6 eV as shown in Fig.4. There is a significant broadening of UV peak with increasing Pt content due to enhancement of 3d(Ni)-5d(Pt) bonding. Chemical disorder enhances the optical response of NiPt alloys nearly one order of magnitude. Our study also shows the fragile magnetic effect on optical response of disordered $Ni_{1-x}Pt_x$ (0.4< x <0.6) binary alloys. We have also shown that ordered $Ni_{50}Pt_{50}$ alloy is non-magnetic, whereas disordered $Ni_{50}Pt_{50}$ is ferromagnetic in nature as shown in Fig.5. The strong environmental dependence of Ni_xPt_{1-x} is the cause of its fragile concentration dependency which changes the electronic structure as well as optical and magnetic response of disordered Ni-Pt systems. Our theoretical predictions agree reasonably well with experimental findings. Our results reveals the fact that both magnetic properties and optical properties in Ni-Pt systems can be tuned using chemical disorder. We anticipate that the theoretical results may provide a valuable reference and open an opportunity to use Ni-Pt alloys an important material for opto-industrial

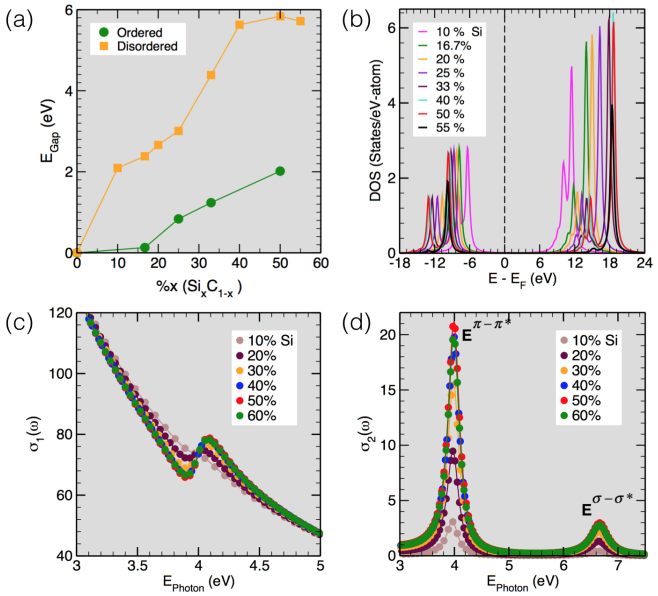

Figure 6: (Color Online) (a) Band gap variation (order and disordered Si_xC_{1-x}), (b) total density of states, (c) real part, and (d) imaginary part of optical conductivity of disordered Si_xC_{1-x} with composition-dependent equilibriumn lattice parameters using TB-LMTO-vLB-ASR. The band gap variation for ordered from Azadeh *et al.*[18] while for disordered case is from TB-LMTO-ASR (using Cambridge recursion library). The maximum in band gap is observed at 50%Si, i.e., Siliphene ($Si_{0.50}C_{0.50}$). We also found that optical conductivity peak at 3.96 eV, in (c) and (d), is in agreement with experimentally observed peak in conductivity at 3.33 eV for 2D ultra-thin SiC [19].

metrology and semiconductor industry.

3.3 Band-gap tuning and optical response of two-dimensional Si_xC_{1-x}

In search of new material, recently, focus has been changed from graphene to other graphene−like 2D materials, with the aim of overcoming the shortage of graphene and broadening its range of applications. Since the honeycomb structure is common to both C and Si, experimentally stable 2D-SiC in honeycomb structure has been synthesized successfully. Recent progress in the fabrication of ultra thin layered 2D-Si_xC_{1-x} makes it an emerging semiconductor attractive to both fundamental research and practical applications. We perform DFT calculations with a LDA-vLB exchange-correlation function to study quantitatively the effect of chemical disorder on the configuration averaged electronic properties and optical response of 2D honeycomb siliphene Si_xC_{1-x}. The LDA and PBE functionals failed to capture important feature in the visible light region, which is important for nanoplasmonic applications. Repulsive effect between the valence band and the conduction band increases with increasing Si content and reduced C−Si bond length. The small bond lengths enhances in-plane $\pi - \pi^*$ repulsion, which helps opening up the band gap. Assuming silicene as the end point of Si_xC_{1-x}) with x=1.0, one would expect the downturn of the mentioned trend beyond 50% (see Fig.6). We have calculated the optical response of disordered 2D Si_xC_{1-x} using the vLB+ASR with composition-dependent

(x) equilibrium lattice parameters. An optical conductivity peak was obtained at 3.96 eV in the low-energy region and at higher energies, we obtained another peak at 6.63 eV as shown in Fig.6. The optical conductivity peak at 3.96 eV is in good agreement with experimental peak at 3.33 eV as reported by Lin *et al.*[19]. We found that silicon can be used to tune the band-gap in Si_xC_{1-x}, which in turn enhances the optical conductivity. The prediction of large optical response in our calculations shows that 2D-Si_xC_{1-x} can be a potential candidate for the solar cell material. The proposed formalism opens up a facile way to band gap engineer material for optoelectronic application.

3.4 Magnetization dynamics in bulk bcc Fe and Fe_xCo_{1-x} alloys : A first-principles augmented space approach

The dynamics and damping of magnetic excitations play a pivotal role in many modern spintronic applications. To date various theoretical techniques have been employed to understand the magnetic excitation phenomena, starting from atomic spin dynamics (UppASD) [20] to frequency-space study of spin-wave excitations. Thermal fluctuation contributes over and above T=0 K. What is now needed a clear description of physical processes that are responsible for spin wave softening over a wide range of composition in chemically disordered alloys. We introduce a formulation using scattering theory and Kubo formalism for understanding the picture. The main objective of this work has been start from a first-principles, density functional approach with as few "parameters" as possible and shed light on the area of scattering of spin-wave excitations by both chemical disorder (impurities, doping and alloying) and structural disorder (defects, local and long-ranged deformations of the lattice). The theoretical methodology we shall use is the combination of the Recursion method and the augmented space method, beyond the usual single site mean field coherent potential approximation (CPA) like approach. We have presented a general method to study magnetization dynamics in chemically disordered alloys (see Appendix for numerical details). The formalism applied to both spectral and response properties should make the errors compatible in different studies. We have demonstrated a successful application to the bulk Fe and Fe_xCo_{1-x} alloys to explain several experimental features in magnon spectra. The necessary exchange parameters are calculated in the the framework of density functional theory (DFT). They were done by means of the Korringa-Kohn-Rostocker Green's function formalism as implemented in the SPRKKR package [21].

The $\vec{q}$-dependent dynamical structure function S($\vec{q}$,ω) is a central quantity for the understanding of magnetism. Fig.7 shows the dynamical structure function $\ll S(\vec{q},\omega) \gg$ convoluted with a Lorenzian function for the disordered, bulk bcc Fe_xCo_{1-x} alloys for three concentrations of x (disorder) with x=0.2, 0.5, 0.8 respectively. The figure displays the calculated dynamical structure factors, for a selection of different $\vec{q}$ vectors varying from 0.0 to 0.9 along the symmetric $\Gamma - Y$ direction i.e. [001] in the reciprocal space of bcc lattice. For low $\vec{q}$ values, the spectral intensity of is high, and decreases with increasing $\vec{q}$. At the same time, the peak width can be seen to increase with increasing energy as well as wave-vector ($\vec{q}$). This is made clear by observing the peaks located at $\vec{q} = 0.1\ \mathring{A}^{-1}$ and $0.8\ \mathring{A}^{-1}$ of three alloy compositions. The broadening of higher energy excitations can be explained by the stronger disorder induced scattering at large $\vec{q}$, i.e. smaller modes. We have study the magnon dispersion of both bulk bcc Fe and

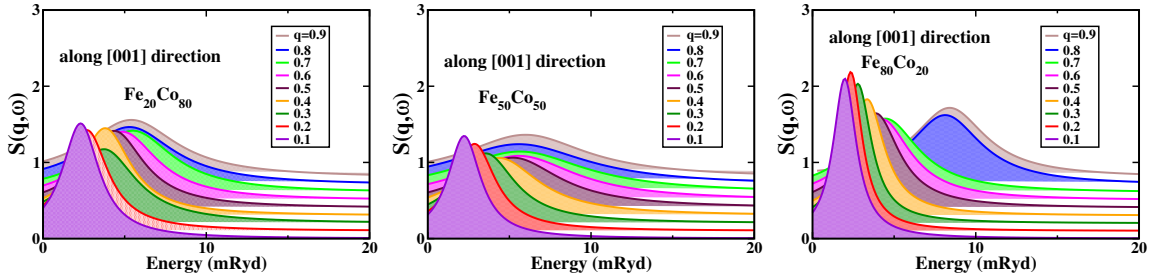

Figure 7: (Color Online) . he dynamical structure factors for a selection of wave-vectors $\vec{q}$ varying from 0.0 to 0.9 along the symmetric $\Gamma - Y$ direction i.e. [001] in the reciprocal space of bcc Fe_xCo_{1-x} alloys with (left) x=0.2 (middle) x=0.5 (right) x=0.8 respectively. In order to identify the peak position the dynamical structure function are convoluted with a Lorentzian function, normalized to unity. Magnon softening is observed for $Fe_{0.2}Co_{0.8}$ alloy at higher $\vec{q}$ values. For low wave-vectors $\vec{q}$, the spectral peaks are strongly intense. The spectral peak width can be seen to increase with increasing energy as well as wave-vector ($\vec{q}$). This leads to more magnon damping at higher $\vec{q}$ values at all concentration

disordered bcc Fe_xCo_{1-x} alloys though our main concern is to study the effect of chemical disorder on the magnetization dynamics of Fe_xCo_{1-x} alloys. Fig.8 shows the magnon dispersion spectrum by identifying the peak positions of the dynamical structure factor $S(\vec{q},\omega)$ for bulk bcc Fe along [001] direction in the first brillouin zone of reciprocal space. We compare our calculated magnon dispersion spectra more explicitly with experimental data on bulk, ferromagnetic bcc Fe by Mook *et al.* [22] and Lynn *et al.* [23]. Mook *et al.* experimentally reported that bulk bcc Fe system has a spin-wave stiffness constant of 280 meV $\mathring{A}^2$. We have calculated the magnon dispersions by identifying the peak positions of the configuration averaged dynamical structure factor $\ll S(\vec{q},\omega) \gg$ along particular directions in reciprocal space of disordered bcc Fe_xCo_{1-x} alloys as shown in Fig.9. After configuration averaging, in order to simplify the identification of the intensity peaks of dynamical structure factor $\ll S(\vec{q},\omega) \gg$, the intensity for each $\vec{q}$ vector is convoluted

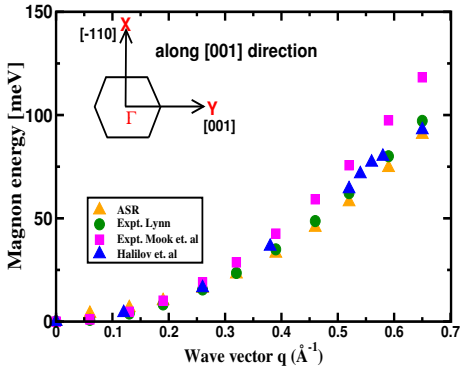

Figure 8: (Color Online) Magnon dispersion spectrum for bulk, bcc Fe along the [001] direction from ASR. For comparison, the experimental spin-wave spectrum of bulk bcc Fe by Lynn [23] and another experimental data corresponding to a spin-wave stiffness constant of D = 280 $\mathring{A}^2$ by Mook *et al.* [22] are also displayed. The blue triangles represent theoretical data by Halilov *et al.* [24]. All comparisin are matches well with ASR.

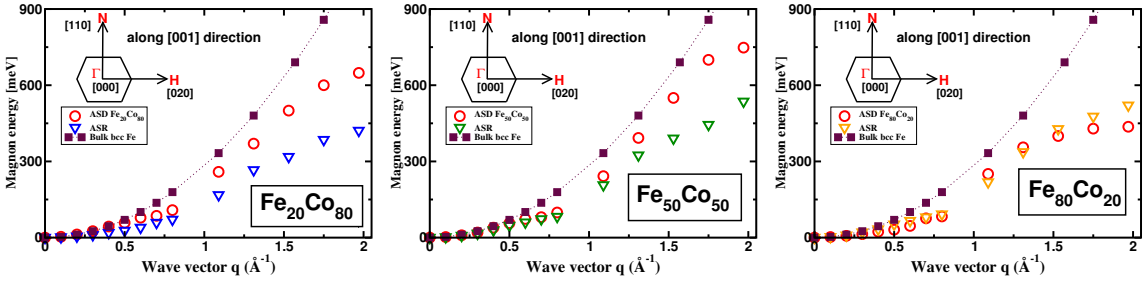

Figure 9: (Color Online) Magnon dispersion spectra for bulk, ferromagnetic and disordered binary (left) $Fe_{20}Co_{80}$, (middle) $Fe_{50}Co_{50}$ and (right) $Fe_{80}Co_{20}$ alloys respectively along the symmetric $\Gamma - Y$ direction i.e. [001] direction with first nearest-neighbour exchange parameters. The magnon spectra from ASR and ASD agrees well. We compare our data the experimental spin-wave spectrum of bulk bcc Fe (corresponding to a spin-wave stiffness constant of 280 meV $\mathring{A}^2$) by Mook *et al.* [22].

with a Lorentzian function, normalized to unity. We find the quadratic dependence upon $\vec{q}$ for the spin wave spectrum of a magnon in the itinerant Heisenberg model of disordered Fe_xCo_{1-x} alloy. $Fe_{80}Co_{20}$ and Bulk Fe have almost similar nature of magnon spectrum. Now the magnon spectrum is gradually soften down if we increase Co content. The large magnon softening with increasing Co content suggests Fe_xCo_{1-x} to be a promising material for recording applications. Literature survey shows a lack of direct available experimental data for disordered $Fe_{20}Co_{80}$ alloy. As a complementary study, we have done atomistic spin dynamics (ASD) simulations by solving Landau-Lifshitz-Gilbert equation with parameters obtained from ab initio multiple scattering theory to compare with the results obtained from augmented space approach.

3.5 Summary of the research and some important results

My research interest during my PhD program includes theoretical studies of the electronic structure, optical and magnetic response of ordered compounds and disordered alloys. We have studied the optical conductivity and dielectric response of disordered, bulk Ni_xPt_{1-x} alloys and disordered, two dimensional Si_xC_{1-x}. This study is based on the density functional approximation and the tight binding linear muffin tin orbitals method. Disorder is taken into account by the "augmented space formalism" which allows us to accurately estimate the effect of disorder both homogeneous disorder as well as inhomogeneous disorder related to shortranged ordering, clustering and segregation. This can be done both in bulk, surfaces and interfaces. We have overcome the defeciency of the LDA and incorporated the vLB-corrected exchange correlations. Our estimation reasonably, successfully agrees with the initial experimental observations. This encourages me to go forward in this area. Specifically, I have been working on the magnetization dynamics and excitation spectra of disordered binary Fe_xCo_{1-x} alloys. We have studied the magnon softening for chemically disordered $Fe_{20}Co_{80}$ alloys in the linear spin wave regime. In parallel, we have been generating the electronic structure of disordered Graphene and Graphinic materials with random vacancies. We have shown how the topology of the Dirac dispersion changes with disorder. We have studied disorder induced lifetime effects in 2D materials. Currently, we are working on the first principles studies of electronic structure and optical

response of chalcopyrite semiconductor $ZnSnP_2$ in collaboration with an experimental group.

List of papers related to thesis:

(i) **Disorder induced lifetime effects in binary disordered systems : a first principles formalism and an application to doped Graphene** : Banasree Sadhukhan, Subhadeep Bandyopadhyay, Arabinda Nayak, Abhijit Mookerjee
Journal Ref : Int. J. Mod. Phys. B (IJMPB) 31 1750218 (2017) ;
DOI: 10.1142/S0217979217502186 ; arXiv:1701.03243

(ii) **Effect of doping on the electronic properties of Graphene and T-graphene : A theoretical approach** : Banasree Sadhukhan, Arabinda Nayak, Abhijit Mookerjee
Journal Ref : Accepted in Indian J Phys (2017) ; DOI: 10.1007/s12648-017-1067-2 ; arXiv:1510.03702

(iii) **Band-gap tuning and optical response of two-dimensional Si_xC_{1-x} : A first-principles real space study of disordered 2D materials** : Banasree Sadhukhan, Prashant Singh, Arabinda Nayak, Sujoy Datta, Duane D. Johnson, Abhijit Mookerjee
Journal Ref : Phys. Rev. B 96, 054203 (2017) , DOI: 10.1103/PhysRevB.96.054203 ; arXiv:1612.07713

(iv) **Effect of disorder on the optical response of NiPt and Ni_3Pt alloys** : Banasree Sadhukhan, Arabinda Nayak, Abhijit Mookerjee
Journal Ref : Computational Materials Science 140, 9 (2017) ;
DOI : http://dx.doi.org/10.1016/j.commatsci.2017.08.003 ; arXiv:1705.06549

(v) **Magnetization dynamics in disordered Fe_xCo_{1-x} alloys : A first-principles augmented space approach and atomistic spin dynamics simulations** : Banasree Sadhukhan, Raghuveer Chimata, Biplab Sanyal, Abhijit Mookerjee
Journal Ref : Communicated ; arXiv:1510.05200

Papers not related to thesis:

(i) **Configuration and self-averaging in disordered systems** : Suman Chowdhury, Debnarayan Jana, Banasree Sadhukhan, Dhani Nafday, Santu Baidya, Tanusri Saha-Dasgupta, Abhijit Mookerjee
Journal Ref : Indian J Phys 90(6), 649 (2016). arXiv:1404.6778

(ii) **Increased metallicity of Carbon nanotubes because of incorporation of extended Stone-Wales defects** : an ab-initio real space approach : Sujoy Datta, Banasree Sadhukhan, Srabani Chakraborty, Chhanda Basu Chaudhuri, Abhijit Mookerjee
Journal Ref : Indian J Phys 89, 165425 (2016).

(iii) **Experimental and first principles studies of electronic structure and optical response of chalcopyrite semiconductor $ZnSnP_2$** : Banasree Sadhukhan, Sukhendu Mukherjee, Tamaghna Maitra, Prashant Singh, Arabinda Nayak, Duane D. Johnson, Abhijit Mookerjee
(Manuscript under preparation)

Acknowledgments

I sincerely acknowledge Prof. Abhijit Mookerjee from SNBNCBS, kolkata for his guidance, active collaboration and very useful discussions. I also like to thank my collaborators Dr. Biplab Sanyal (Department of Physics and Astronomy, Uppsala University, Sweden), Prashant Singh (Ames Laboratory, Iowa State University, USA), Sujoy Dutta, Subhadeep Bandyopadhyay, Sukhendu Mukherjee, Tamaghna Maitra for useful discussions.

APPENDIX

.1 Kubo Formalism and Real Space Recursion.

In Recursion, we express the Kubo response of the valence electrons to optical disturbance in a form so that the necessary correlation functions can also be expressed through a generalized recursion technique [25].

$$\langle j^{\mu}(t)\rangle = \int_{-\infty}^{\infty} dt' \sum_{\nu} \chi^{\mu\nu}(t-t')A^{\nu}(t') \tag{2}$$

where

$$\chi^{\mu\nu}(t-t') = \frac{i}{\hbar}\Theta(t-t')\langle G|[j^{\mu}(t), j^{\nu}(t')]|G\rangle$$

where $|G\rangle$ is the ground state. In lattices with cubic symmetry, $\chi^{\mu\nu} = \chi\delta_{\mu\nu}$. The Fluctuation-Dissipation Theorem relates the imaginary part of the Laplace transform of the generalized susceptibility $\chi''(\omega)$ to the current-current correlation function :

$$\begin{aligned}\chi''(\omega) &= \frac{1}{2\hbar}\left[\text{-}1 - \exp(-\beta\hbar\omega)\right]\ S(\omega) \\ \text{where} & \\ S(\omega) &= \int_0^\infty dt\ \exp(i\omega t)\ \langle G|j(t)j(0)|G\rangle\end{aligned}$$

The correlation function can be obtained most directly using the generalization of the recursion method. This has been described in detail by Viswanath and Müller [25, 26]. Analogous to the standard Recursion for single particle propagators, we generate a new basis from a three term recurrence :

(i) $|f_{-1}\rangle = 0\ ;\ |f_0\rangle = j(0)|G\rangle$

(ii) We generate the rest of the basis recursively :

$$|f_{m+1}\rangle = H|f_m\rangle - \alpha_m|f_m\rangle - \beta_m^2|f_{m-1}\rangle \quad m = 0, 1, 2\ldots$$

(iii) Mutual orthonormality leads to :

$$\alpha_m = \frac{\langle f_m|H|f_m\rangle}{\langle f_m|f_m\rangle} \quad \text{and} \quad \beta_m^2 = \frac{\langle f_m|f_m\rangle}{\langle f_{m-1}|f_{m-1}\rangle}$$

We can now expand any wave ket $|\psi\rangle$ in terms of the orthogonal basis just generated :

$$|\psi(t)\rangle \quad = \quad \sum_{m=0}^{\infty} C_m(t)|f_m\rangle$$

$$i\frac{d}{dt}C_m(t) = C_{m-1}(t) + \alpha_m C_m(t) + \beta_{m+1}^2 C_{m+1} \tag{3}$$

with C_{-1}=0 and $C_m(0) = \delta_{m,0}$. Taking Laplace transform we get,

$$(z - \alpha_m)C_m(z) + i\delta_{m,0} = C_{m-1}(z) + \beta_{m+1}^2 C_{m+1}(z) \tag{4}$$

Recursive steps now give us :

$$C(z) = C_0(z) = \cfrac{-i}{z - \alpha_0 - \cfrac{\beta_1^2}{z - \alpha_1 - \cfrac{\beta_2^2}{z - \alpha_2 - \ldots}}}$$

So that :

$$S(\omega) = 2\lim_{\delta\to 0}\ \Re e\ C(\omega + i\delta) \tag{5}$$

.2 Disorder and the Augmented Space approach.

We model local disorder with associating with the tight-binding Hamiltonian elements a set of random parameters $\{n_m\}$. For binary alloying, for example, n_m takes the values 0 and 1 with probabilities x and y.

$$[t]H = \sum_m \left(\epsilon_A n_m + \epsilon_B(1-n_m)\right)\mathcal{P}_m + \sum_m \sum_{m'} \Big\{ t_{AA} n_m n_{m'} + t_{BB}(1-n_m)(1-n_{m'}) \text{-} \ldots + t_{AB}\left\{n_m(1-n_{m'}) + (1-n_m)n_{m'}\right\} \text{-} \Big\} \mathcal{T}_{mm'} \quad (6)$$

with the projection and transfer operators $\mathcal{P}_m$ and $\mathcal{T}_{mn} \in \mathcal{H}$. Following the ideas of measurement theory, the prescription is to replace the random parameters by the operator $\tilde{N}_m$ [7] whose spectrum are the possible results of measurement and whose spectral density is the probability of obtaining these results. For example, if n_m takes the values 0 and 1 with probabilities x and y then $\tilde{N}_m$ is of rank 2 with a representation :

$$\begin{pmatrix} x & \sqrt{xy} \\ \sqrt{xy} & y \end{pmatrix} \qquad \tilde{N}_m \in \mathcal{Z}_m^{(2)}$$

The basis used here is $|\mathcal{C}_0^m> = \sqrt{x}|0^m> + \sqrt{y}|1^m>$ and $|\mathcal{C}_1^m> = \sqrt{y}|0^m> - \sqrt{x}|1^m>$

The full configuration space is $\mathcal{Z} = \prod_m^{\otimes} \mathcal{Z}_m^{(2)}$ and the augmented Hamiltonian in $\Psi = \mathcal{Z} \otimes \mathcal{H}$ is :

$$\widetilde{H} = \sum_m \Big(\epsilon_A \tilde{N}_m + \epsilon_B(\tilde{I} - \tilde{N}_m)\Big) \otimes \mathcal{P}_m + \sum_m \sum_{m'} \Big(t_{AA} \tilde{N}_m \otimes \tilde{N}_{m'} + t_{BB}(\tilde{I} - \tilde{N}_m) \otimes (\tilde{I} - \tilde{N}_m) + t_{AB} \Big\{ \tilde{N}_m \otimes (\tilde{I} - \tilde{N}_{m'}) + (\tilde{I} - \tilde{N}_m) \otimes \tilde{N}_{m'} \Big\}] \otimes \mathcal{T}_{mm'} \quad (7)$$

The Augmented Space Theorem [7] tells us that the configuration average of any function of $\{n_m\}$ is :

$$\ll F(\{n_m\}) \gg = \langle G \otimes \{\mathcal{C}_0\} | \widetilde{F}(\{\tilde{N}_m\}) | G \otimes \{\mathcal{C}_0\} \rangle \quad (8)$$

With $|\{\mathcal{C}_0\}\rangle = \prod^{\otimes} |\mathcal{C}_0^m\rangle$ and $\widetilde{F} \in \mathcal{Z} \otimes \mathcal{H} = \Psi$

Now disorder can be combined with Recursion using the ideas of Augmented Space with all operators and states in $\Psi = \mathcal{Z} \otimes \mathcal{H}$ It follows that :

$$\ll S(\omega) \gg = \int_0^{\infty} dt \exp(i\omega t) \left\langle G \otimes \{\mathcal{C}_0\} | \tilde{j}(t)\ \tilde{j}(0) | G \otimes \{\mathcal{C}_0\} \right\rangle \quad (9)$$

We calculate this using Generalized Recursion in the full augmented space Ψ. The dielectric function and optical conductivity are related :

$$\ll \epsilon_2(\omega) \gg = 4\pi \lim_{\delta \to 0} \frac{\ll \mathrm{S}(z) \gg}{z^2} = \frac{\omega}{4\pi} \ll \sigma(\omega) \gg \quad (10)$$

.3 The Optical Current.

The calculations begin with a thorough electronic structure calculation using the tight-binding linear muffin-tin orbitals method. The technique, like many others, is based on the density functional theory, where the energetics depends entirely upon the charge and spin densities. However, the current operator which is characteristic of an excited electron : excited optically, electronically or magnetically, is described by transition probabilities which depend upon the wave-function. The wave-functions are expressed as linear combinations of the linearized basis functions : the muffin-tin orbitals.

$$\Psi(\vec{r}) = \sum_{RL} c_{RL} \left[\phi_{RL}(\vec{r}) + \sum_{RL,R'L'} h_{RL,R'L'} \ \phi'_{R'L'}(\vec{r}) \right] \tag{11}$$

TB-LMTO-ASR calculations were done self-consistently and non-relativistically for a given geometry till the "averaged relative error" between the converged final and the previous iteration charge density and energy is reached. Nowhere do we use lattice translation symmetry so that Bloch's theorem plays no role.

The calculations begin with a thorough electronic structure calculation using the tight-binding linear muffin-tin orbitals method. The technique, like many others, is based on the density functional theory, where the energetics depends entirely upon the charge and spin densities. However, the current operator which is characteristic of an excited electron : excited optically, electronically or magnetically, is described by transition probabilities which depend upon the wave-function. The wave-functions are expressed as linear combinations of the linearized basis functions of the LMTO. The wave-function representation in the LMTO basis is :

$$\Psi(\vec{r}) \ = \ \sum_{RL} c_{RL} \left[\phi_{RL}(\vec{r}) + \sum_{nL,n'L'} h_{nL,n'L'} \ \phi'_{n'L'}(\vec{r}) \right] \tag{12}$$

where $\phi'_{nL} = \partial\phi(\vec{r}, E)/\partial E$

The coefficients c_{nL} are available from our TB-LMTO secular equation. To obtain the currents we follow the procedure of Hobbs *et al.* [27]. The optical current operator is given by :

$$j^{\mu} = \sum_{RL} J^{\mu}_{RL,RL} \mathcal{P}_{RL} + \sum_{RL} \sum_{R'L'} J^{\mu}_{RL.R'L'} \mathcal{T}_{RL,R'L'} \tag{13}$$

$$\begin{aligned} J^{\mu}_{RL,RL} &= V^{(1),\mu}_{RL,RL} \\ J^{\mu}_{RL,R'L'} &= \sum_{R''L''} \left\{ V^{(2),\mu}_{RL,R''L''} h_{R''L'',R'L'} + \ldots h_{RL,R''L''} V^{(3),\mu}_{R''L'',R'L'} \sum_{R''L''} V^{(4),\mu}_{R''L",R''',L'''} h_{R'''L''',R'L'} \right\} \end{aligned}$$

where,

$$V^{(1),\mu}_{RL,RL'} = \int_{r<s_R} d^3\vec{r}\ \phi^*_{RL'}(\vec{r})(-i\nabla^\mu)\phi_{RL}(\vec{r})$$
$$V^{(2),\mu}_{RL,RL'} = \int_{r<s_R} d^3\vec{r}\ \widehat{\phi}^*_{RL'}(\vec{r})(-i\nabla^\mu)\widehat{\phi}_{RL}(\vec{r})$$
$$V^{(3),\mu}_{RL,RL'} = \int_{r<s_R} d^3\vec{r}\ \phi^*_{RL'}(\vec{r})(-i\nabla^\mu)\widehat{\phi}_{RL}(\vec{r})$$
$$V^{(4),\mu}_{RL,RL'} = \int_{r<s_R} d^3\vec{r}\ \widehat{\phi}^*_{RL'}(\vec{r})(-i\nabla\mu)\widehat{\phi}_{RL}(\vec{r})$$

We have followed the prescription of Hobbs *et al.*[27] to evaluate the integrals above. For details we again refer to reader to the above reference. We should note that we have so far not introduced the idea of reciprocal space. We expect our methodology to be applicable to situations w The ASR method is a real-space technique for treating random disorder of alloys. Recursion [25, 26] needs a countable basis $\{|n>\} \in Z^d$ which is provided by the TB-LMTO-ASA basis with R labelling the atomic positions $\vec{R}_n$.

.4 Spin transport at low temperatures.

We analyse spin transport in ferromagnetic alloys. We begin with a ferromagnetic sea as our unperturbed state. A spin flip is an excitation or fluctuation in that state. We re-interpret the XXZ Heisenberg Hamiltonian with a random distribution of the exchange parameters $J(\vec{R}-\vec{R'})$ in terms of creation and annihilation operators of such fluctuations and their 'transfer' through the lattice :

$$H = -\sum_{\vec{R}}\sum_{\vec{R'}} J(\vec{R}-\vec{R'})\left(a^\dagger_{\vec{R}}a_{\vec{R'}} + a^\dagger_{\vec{R'}}a_{\vec{R}} + \Delta\ n_{\vec{R}}\ n_{\vec{R'}}\right) \tag{14}$$

where Δ is the anisotropic exchange parameter describing magnon-magnon interaction, $J(\vec{R}-\vec{R'})$ is the strength of the exchange interaction. $a^\dagger_{\vec{R}}$, $a_{\vec{R}}$ are the magnon creation, annihilation operators respectively and $n_R = a^\dagger_{\vec{R}}a_{\vec{R}}$. The excitations described in this model : spin waves or magnons can be envisaged as spin-patterns against a uniform spin background moving on the underlying lattice. The Hilbert space $\mathcal{H}$ (H $\in \mathcal{H}$) is spanned by these "spin pattern" states. We begin with the model of ion cores sitting on the lattice immersed in a bonding sea of electron provided by atoms where they bond to form a solid. Here we put disorder in the exchange terms to make the alloy chemically impure. The randomness can be introduced in the exchange parameter through a local, binary random variable $n_{\vec{R}}$ ($\vec{R}$ can be occupied by A or B type of atom) taking the values 0 and 1 with probabilities x and $y = 1-x$:

$$J(\vec{\chi}) = J^{AA}(\vec{\chi})n_{\vec{R}}n_{\vec{R}+\vec{\chi}} + J^{BB}(\vec{\chi})(1-n_{\vec{R}})(1-n_{\vec{R}+\vec{\chi}}) + J^{AB}(\vec{\chi})\left(n_{\vec{R}}(1-n_{\vec{R}+\vec{\chi}}) + (1-n_{\vec{R}})n_{\vec{R}+\vec{\chi}}\right)$$

The model is very similar to that described by the Bose-Hubbard Hamiltonian, with the exchange energy $J(\vec{R}-\vec{R'})$ playing the role of the hopping overlap which allows the excitations to propagate through the lattice. We are initially not interested in the low temperature regime, so Δ is small and in the first instance we shall neglect it in linear spin wave regime (LSWT). Here in our case we take at T=0 temperature for spin transport.

References

[1] D Biava *et al. Phys. Rev. B* **72** 113105 (2005), D. Kodderitzsch, H. Ebert, D. A. Rowlands, and A. Ernst, *New J. Phys.* **9**, 81 (2007).

[2] A Zunger *et al. Phys. Rev. Lett* **65** 353 (1990)

[3] Y Wang *et al. Phys. Rev. Lett* **75** 2867 (1995)

[4] R Mills and P Ratanavararaksa *Phys. Rev. B* **18** 5291 (1978)

[5] S Ghosh, P Leath, and M Cohen *Phys. Rev. B* **66** 214206 (2002)

[6] A. Mookerjee, in: A. Mookerjee, D.D. Sarma (Eds.), Electronic Structure of Clusters, Surfaces and Disordered Solids, Taylor Francis, 2003

[7] A Mookerjee *J. Phys. C: Solid State Phys* **6**, L205 (1973)

[8] A. Mookerjee *J. Phys. C* **6**, 1340 (1973)

[9] A. Mookerjee *J. Phys. C* **8**, 1524 (1974)

[10] A. Mookerjee *J. Phys. C* **8**, 2688 (1976)

[11] A. Mookerjee *J. Phys. C* **9**, 1225 (1976)

[12] von Barth U. and Hedin L., *J. Phys. C* **5** 1629 (1972)

[13] R. van Leeuwen and E. J. Baerends, *Phys. Rev. B*A **49**, 2421 (1994).

[14] R. Kubo *J. Phys. Soc. Jpn* **12**, 570 (1957)

[15] D. A Greenwood *Proc. Phys Soc* **71**, 585 (1958)

[16] Yu Liu *et al. Phys. Rev. Lett* **108** 225505 (2012)

[17] T. B. Massalski, *ASM International, Materials Park, Ohio* **2844** (1990)

[18] M.S. Sharif Azadeh, A. Kokabi, M. Hosseini, M. Fardmanesh, *Micro & Nano Letters* **6(8)** 582 (2011); DOI: 10.1049/mnl.2011.0195

[19] S. S. Lin *J. Phys. Chem. C* **116** 6 (2012); DOI: 10.1021/jp210536m

[20] http://physics.uu.se/forskning/materialteori/pagaende-forskning/uppasd/

[21] *The Munich SPR-KKR package, version 6.3*, H. Ebert *et al*, http://ebert.cup.uni-muenchen.de/SPRKKR; H. Ebert, D. Ködderitzsch and J. Minár, Rep. Prog. Phys. **74**, 096501 (2011).

[22] H. A. Mook and R. M. Nicklow, *Phys. Rev. B* **7**, 336 (1973) DOI : https://doi.org/10.1103/PhysRevB.7.336

[23] J. W. Lynn, *Phys. Rev. B* **11**, 2624 (1975). DOI : https://doi.org/10.1103/PhysRevB.11.2624

[24] S. V. Halilov, A. Y. Perlov, P. M. Oppeneer and H. Eschrig , *Europhys. Lett.*, **39(1)** (1997).

[25] V. Viswanath and G. Müller, sl The Recursion Method, Applications to Many-Body Dynamics Germany : Springer-Verlag (1994)

[26] V. S. Viswanath, and G Müller, J. Appl. Phys. **67**, 5486 (1990).

[27] D. Hobbs, E. Piparo, R. Girlanda, and M. Monaca, J. Phys. Condens. Matter **7** 2541 (1995).